

Solar cycle signal in a general circulation and chemistry model with internally generated quasi-biennial oscillation

H. Schmidt,¹ G. P. Brasseur,^{2,3} and M. A. Giorgetta¹

Received 27 May 2009; revised 20 November 2009; accepted 10 December 2009; published 17 April 2010.

[1] Simulations with the HAMMONIA general circulation and chemistry model are analyzed to improve the understanding of the atmospheric response to solar cycle variations and the role of the quasi-biennial oscillation of equatorial winds (QBO) for this response. The focus is on the Northern Hemisphere winter stratosphere. Owing to the internally produced QBO, albeit with a too short period of 24 months, the model is particularly suited for such an exercise. The simulation setup with only solar and QBO forcing allows an unambiguous attribution of the simulated signals. Two separate simulations have been performed for perpetual solar maximum and minimum conditions. The simulations confirm the plausibility of dynamical mechanisms, suggested earlier, that propagate the solar signal from the stratopause region downward to the troposphere. One feature involved in this propagation is a response maximum of temperature and ozone in the lower equatorial stratosphere. In our model, this maximum appears as a pure solar signal independent of the QBO and of other forcings. As observed, the simulated response of the stratospheric polar vortex to solar cycle forcing depends on the QBO phase. However, in the model this is statistically significant only in late winter. The simulation for early and mid winter suffers probably from a too strong internal variability of the polar vortex in early winter.

Citation: Schmidt, H., G. P. Brasseur, and M. A. Giorgetta (2010), Solar cycle signal in a general circulation and chemistry model with internally generated quasi-biennial oscillation, *J. Geophys. Res.*, 115, D00I14, doi:10.1029/2009JD012542.

1. Introduction

[2] The response of stratospheric temperature, winds and chemical species to the variability of solar radiation associated with the 11 year solar cycle has been intensively studied in the past, both through the analysis of observations and numerical simulations. Many details of the response and the physical mechanisms involved remain, however, unclear. One reason is the difficulty to disentangle in the observations solar signals from those related to the quasi-biennial oscillation (QBO) of equatorial zonal winds [Lee and Smith, 2003; Smith and Matthes, 2008]. The shortness of most observational time series with respect to the 11 year periodicity of the solar cycle aggravates this problem. Soukharev and Hood [2006], for example, have calculated fairly different ozone signals from time series observed during different periods by three different satellite instruments. Intensive research has focussed in the recent years on the role of dynamical feedbacks in the response to solar variability during Northern Hemisphere (NH) winter. This region, however, is characterized by large internal variability, and it is affected not only by solar variability and the QBO but also by other types of forcing including increasing greenhouse gas concentrations,

volcanic eruptions and variations in sea surface temperature (SST) variations (in particular those related to El Niño–Southern Oscillation (ENSO)). Under these conditions, numerical modeling is a valuable tool for the interpretation of observations and for testing hypotheses on mechanisms involved in the response. This study analyzes simulations with the Hamburg Model of the Neutral and Ionized Atmosphere (HAMMONIA) [Schmidt *et al.*, 2006], a three-dimensional general circulation and chemistry model, including imposed solar cycle variability and an internally produced QBO, but neglecting other external forcings like those mentioned above.

[3] One persistent feature in different observational analyses is a response structure with two maxima in both equatorial ozone and temperature [e.g., Crooks and Gray, 2005; Labitzke *et al.*, 2002; Randel and Wu, 2007]. The upper stratospheric maximum is commonly attributed to direct radiative effects on heating and photochemistry while the lower stratospheric maximum is thought to be related to changes in equatorial upwelling. Kadera and Kuroda [2002] suggested a mechanism to explain this lower stratospheric response that involves planetary wave–mean flow interaction in mid to high latitudes. Several recent model simulations reproduce such a maximum in the lower stratosphere. But the reasons for this success are diverse. In simulations with several models, this secondary maximum appears only or is enhanced in transient experiments with time varying solar irradiance and SSTs [Austin *et al.*, 2008]. Marsh and Garcia [2007] have shown that the ENSO phase was weakly correlated with the solar cycle in the recent decades. In their simulations with the Whole Atmosphere Community Climate

¹Max Planck Institute for Meteorology, Hamburg, Germany.

²Climate Service Center, Hamburg, Germany.

³ESSL, National Center for Atmospheric Research, Boulder, Colorado, USA.

Model (WACCM) this correlation contributes to the secondary maximum. As, according to *Kodera and Kuroda* [2002], the equatorial lower stratospheric response is linked to higher-latitude processes, which depend on the QBO (see below), a QBO dependence of the secondary maximum seems plausible. In 2D-model simulations by *McCormack et al.* [2007] the secondary maximum occurs only when a QBO is present. In the same simulations, the QBO itself is modulated by the solar cycle: During solar maximum, a shorter duration of the westerly QBO phase is simulated than during solar minimum. The same feature was analyzed from observations by *Salby and Callaghan* [2000]. *Hamilton* [2002], however, reports that the available time series is too short for an unambiguous attribution of this change in the QBO period.

[4] Another important feature of the stratospheric response is the interdependence of solar cycle and QBO signals that can be identified in particular in stratospheric north polar winter temperatures [e.g., *Labitzke*, 1987; *Labitzke and van Loon*, 1988; *Labitzke*, 2005]. It is commonly assumed that both QBO and solar variability modulate stratospheric winds in the winter hemisphere, which modifies the propagation conditions for planetary waves and feeds back on winds and temperature. It has been suggested by *Holton and Tan* [1980, 1982] that, during the westerly QBO phase, the polar vortex is stronger and colder than during the easterly phase. Since then, several authors have shown that this effect holds mainly for early winter months and also depends on the solar cycle phase being significant only during solar minimum [e.g., *Labitzke and van Loon*, 1988; *Naito and Hirota*, 1997; *Gray et al.*, 2001]. Analyzing ECMWF reanalysis and operational data from 1958–2006, *Lu et al.* [2008] have confirmed these findings and also reported a yet unexplained decadal-scale variation in the Holton–Tan relationship that apparently does not depend on the solar cycle. *Camp and Tung* [2007a] have analyzed NCEP–NCAR reanalysis data and singled out the combination of solar minimum and QBO west phase as producing the least-perturbed state of the northern polar winter stratosphere with solar minimum and QBO east phase both adding a perturbation leading to a warming. The dependence of the QBO–polar vortex relationship on the phase of the solar cycle can also be interpreted as a dependence of the solar signal on the QBO phase. *Labitzke and van Loon* [1988] found a positive correlation between solar cycle and observed stratospheric north pole temperature only in the westerly QBO phase. This finding has been confirmed since then but, to our knowledge, not yet satisfactorily reproduced in model simulations with internally produced QBO. *Matthes et al.* [2004] simulated a QBO–solar cycle relation for NH winter similar to the corresponding observed relation but with relatively weak amplitude using a model setup with prescribed (observed) QBO.

[5] A tropospheric response to solar cycle variability has been identified in several parameters [e.g., *Gleisner and Thejll*, 2003; *Kodera and Shibata*, 2006; *van Loon et al.*, 2007; *Camp and Tung*, 2007b]. A variety of mechanisms to explain these tropospheric signals has been proposed and supported by model studies [e.g., *Haigh*, 1999; *Haigh et al.*, 2005; *Matthes et al.*, 2006; *Meehl et al.*, 2008]. Those suggestions include downward propagation from the stratosphere and in situ generation. In a recent study with a coupled middle atmosphere–ocean model, *Meehl et al.* [2009] have

shown that both mechanisms may act together to enhance the solar signal in the tropical Pacific. It has also been suggested from simulations with a simplified general circulation model [*Berg et al.*, 2007] that a solar cycle like response in the NH winter stratosphere may be produced by forcing a model with the observed upper tropospheric solar cycle response in geopotential height. Hence, as for the lower stratospheric secondary maximum (see above), it remains unclear to what extent feedbacks via the troposphere are important for the stratospheric solar cycle signal.

[6] Recently, complex middle atmosphere chemistry climate simulations of the past five decades including most known forcings have been performed in the context of the CCM Validation Activity for SPARC (CCMVAL) [e.g., *Eyring et al.*, 2006, 2008]. Such simulations are extremely important because they allow a direct comparison with observations. On the other hand, it is useful to perform simulations with models of similar complexity but applying only selected types of forcing to allow an easier attribution of the simulated signals. This is the rationale of the present study in which it is attempted to improve our understanding of the solar cycle influence on the stratosphere under different QBO phases.

[7] Section 2 of this paper provides a description of the HAMMONIA and of the simulation setup. In section 3, the simulated solar signal is analyzed without distinguishing between the QBO phases. The main focus is on the secondary response maximum in the lower equatorial stratosphere. It is shown that a relatively weak secondary maximum may appear as a pure solar signal with climatological SSTs (i.e., excluding ENSO variability) and that the mechanism as suggested by *Kodera and Kuroda* [2002] is likely to explain this feature. In section 4, the QBO dependence of the stratospheric NH winter response is analyzed. Section 4 starts with an evaluation of the simulated QBO. A summary of the results and conclusions are presented in section 5.

2. Model Description and Simulation Setup

[8] The Hamburg Model of the Neutral and Ionized Atmosphere (HAMMONIA) is a general circulation and chemistry model that extends from the surface to the thermosphere with the upper lid at $1.7 \cdot 10^{-5}$ hPa (~ 250 km). It is based on the middle atmosphere version (MAECHAM5) [e.g., *Manzini et al.*, 2006] of the ECHAM5 general circulation model [*Roeckner et al.*, 2006], extended by several parameterizations accounting for upper atmosphere processes and coupled to the MOZART3 chemistry mechanism [*Kinnison et al.*, 2007]. Photodissociation rates are calculated in 156 spectral bands from 120 to 780 nm. Heating rates in the middle atmosphere are derived from the same spectral resolution. A detailed description and evaluation of the HAMMONIA, and results of solar cycle experiments are presented by *Schmidt et al.* [2006] and *Schmidt and Brasseur* [2006]. Further, HAMMONIA simulations have been analyzed, for example, with respect to the solar rotational variation [*Gruzdev et al.*, 2009], CO₂ doubling [*Schmidt et al.*, 2006], atmospheric tides [*Achatz et al.*, 2008; *Yuan et al.*, 2008], and waves in the mesopause region [*Offermann et al.*, 2007, 2009].

[9] With respect to the description given by *Schmidt et al.* [2006], the model has been modified slightly for the simu-

lations presented here. As in the work by *Schmidt et al.* [2006], the HAMMONIA is run with a triangular truncation at wave number 31 (T31) but with 119 vertical layers instead of 67. While the vertical resolution remained unchanged above 0.03 hPa, it has been increased considerably in the upper troposphere and stratosphere where the layer thickness is now of about 800 m. This fine vertical resolution allows for an internal simulation of a stratospheric quasi-biennial oscillation. Details on the simulation of the QBO with the MAECHAM5 model have been presented by *Giorgetta et al.* [2006]. The structure of the QBO in equatorial zonal wind simulated by the HAMMONIA is presented in section 4.1.

[10] Although the model extends into the thermosphere, this study concentrates on the stratosphere and lower mesosphere. Differences between the current simulations and those presented by *Schmidt et al.* [2006] are small for higher altitudes where the vertical resolution remained unchanged and the QBO influence is weak.

[11] In order to keep the simulated QBO comparable with that simulated with MAECHAM5 by *Giorgetta et al.* [2006], the same parameters of the Hines gravity wave scheme [*Hines, 1997a, 1997b*] have been used. However, this implies a few modifications with respect to the simulations described by *Schmidt et al.* [2006]. Here, no dependence of the gravity wave source strength on fronts [*Charron and Manzini, 2002*] has been considered; instead, the uniform background gravity wave source strength has been increased to the values used by *Giorgetta et al.* [2006].

[12] Changes in simulated climatological mean values of temperature, winds and most chemical species with respect to fields presented by *Schmidt et al.* [2006] are small except for those regions directly influenced by the QBO. A similarly small net effect of the QBO has been shown in other studies with models of the ECHAM family [*Giorgetta et al., 2006; Punge and Giorgetta, 2008*]. Hence, no updated climatological fields are presented here. The variability in Northern Hemisphere winter, however, increases significantly with the inclusion of the QBO. This effect will be discussed in section 3.2, differences between the QBO phases in section 4.3. An exceptionally large net difference between the simulations with and without QBO can be seen in the water vapor content of the middle atmosphere. The increase of the vertical resolution in the tropopause region has led to a considerable decrease of cross-tropopause flux of water vapor into the stratosphere. While the earlier simulations [*Schmidt et al., 2006*] overestimate stratospheric water vapor in comparison to observations, the present version of the model exhibits an underestimation with annual average maximum volume mixing ratios between about 1.9 and 5.3 ppmv.

[13] As in the experiments described by *Schmidt et al.* [2006], no transient solar cycle has been considered in the current experiment. Instead, we have performed two simulations for perpetual solar minimum and solar maximum conditions. In both cases, 42 years have been simulated. Initial conditions were taken from the respective simulations by *Schmidt et al.* [2006]. However, owing to the initial trend in water vapor, only the last 35 years were used in the analysis. Solar maximum and minimum radiative flux has been chosen as by *Schmidt et al.* [2006]: Fluxes are representative of conditions as in September 1986 (solar minimum, average of 69 sfu (solar flux units, units of the F10.7 cm flux)) and

in November 1989 (solar maximum, 235 sfu). The extreme ultraviolet (EUV) radiation is calculated according to *Richards et al.* [1994]. UV and visible parts of the spectrum were provided by J. Lean [see *Lean, 2000*].

[14] In the second part of the analysis, the simulated NH winters have been grouped into those dominated by westerly and easterly QBO winds (denoted as QBO-w and QBO-e, respectively, in the following). Winters with January-February mean equatorial zonal winds at 30 hPa of above 5 m/s and below -5 m/s have been selected as QBO-w and QBO-e winters, respectively. In most earlier studies, lower altitudes between 50 and 40 hPa were adopted to define the QBO criterion. However, our criterion separates the available 35 simulated years for solar maximum and minimum into groups of almost equal size with 15 to 18 winters belonging to each QBO phase. As the simulated QBO does not reach as low down in the atmosphere as the observed one, lower-level criteria would reduce the number of winters available for analysis in each group.

3. Analysis of the Solar Cycle Signal Not Accounting for the QBO Phase

[15] An analysis of the solar cycle signal without distinguishing the QBO phases allows to assess the “pure” response of the atmosphere to solar forcing and a comparison to many observational analyses that also do not account for the QBO phases. This is in particular the case for analyses of satellite data where time series are in general very short. We do however compare our results to earlier simulations without QBO [*Schmidt et al., 2006; Schmidt and Brasseur, 2006*] to assess a possible net influence of the QBO on the solar signal.

3.1. Annual Average Response

[16] Figures 1 and 2 show the simulated annual and zonal average responses of temperature and ozone to solar cycle forcing. Please note, to facilitate comparison with other studies, results have been normalized to a forcing of 100 sfu. To obtain the actual difference between the simulations for solar maximum and minimum, the numbers in Figures 1 and 2 have to be multiplied with 1.66. Other studies have assumed other differences between solar maximum and solar minimum. Mesosphere and lower thermosphere are included in Figures 1 and 2 for completeness. The results in this region do not differ significantly from those presented and discussed by *Schmidt et al.* [2006]. Here, the focus is on the stratosphere.

[17] The temperature difference between solar maximum and minimum is significantly positive in most parts of the stratosphere. Values above 0.5 K/100 sfu (with a maximum of 0.75 K/100 sfu) occur in the stratopause region. A weak maximum of about 0.25 K/100 sfu is simulated in the lowermost equatorial stratosphere. These upper and lower stratospheric features will be called primary and secondary maximum in the following. A significant negative response is only simulated in high northern latitudes below 10 hPa. This response minimum is due to the dynamical response in NH winter (see section 3.2). In the summer hemispheres, no negative temperature effects have been simulated.

[18] *Randel et al.* [2009] have analyzed the stratospheric temperature response from radiosonde and satellite (SSU and MSU) observations. They assume a difference of 125 sfu between solar maximum and minimum. SSU data show sig-

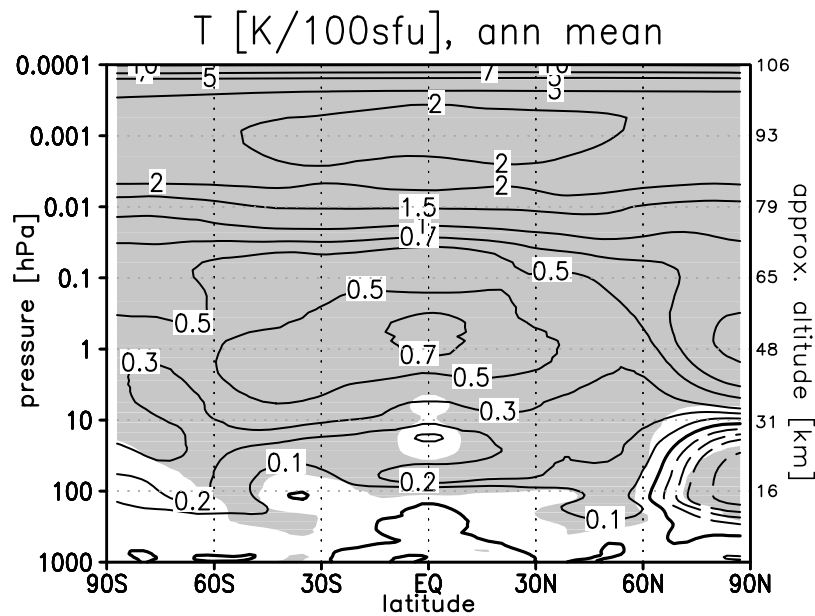


Figure 1. Annual and zonal average temperature response (K/100 sfu) to solar forcing. The response has been normalized to 100 solar flux units (sfu). To obtain the actual difference between the simulations for solar maximum and minimum, the result has to be multiplied by 1.66. Gray shading marks the regions where the statistical significance of the difference is larger than 95%.

nificant positive responses for all stratospheric heights at low latitudes and above ~ 40 km (~ 3 hPa) at high latitudes poleward of 60°N/S . The equatorial response reaches more than 1K in the upper stratosphere. Both radiosonde and satellite data show a response of about 0.4 to 0.5 K above about ~ 80 hPa. According to the SSU data this may be a weak local maximum. Reanalysis data that have been analyzed, for example, by NCEP/NCAR [Labitzke *et al.*, 2002], ECMWF

ERA40 [Crooks and Gray, 2005], and Frame and Gray [2010], who present an update and a slight correction of the earlier study by Crooks and Gray [2005]) indicate a more structured response and in particular more distinct secondary maxima. Randel *et al.* [2009], however, caution against the interpretation of these data sets due to inherent discontinuities.

[19] Also, the simulated ozone response is significantly positive in most parts of the stratosphere. A maximum of

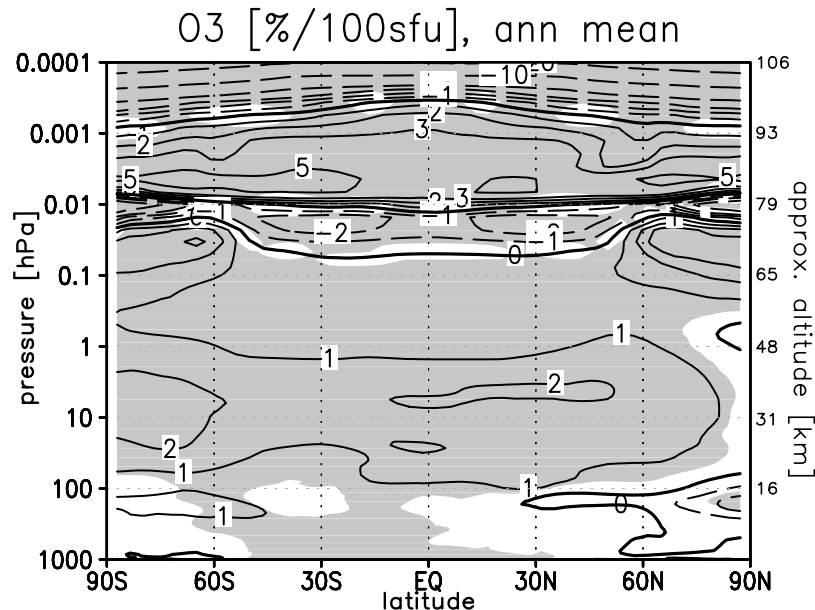


Figure 2. Annual and zonal average relative response in ozone volume mixing ratio (%/100 sfu) to solar forcing. Results have been normalized as in Figure 1. Gray shading marks the regions where the statistical significance of the difference is larger than 95%.

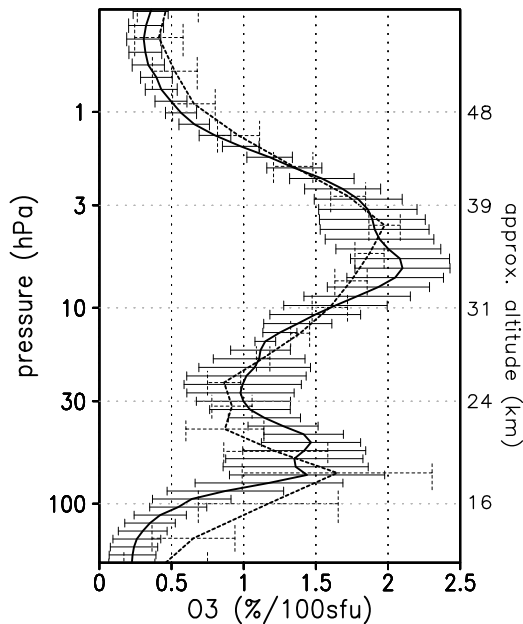


Figure 3. Annual and zonal average equatorial relative response in ozone volume mixing ratio (%/100 sfu) to solar forcing. Solid line denotes model version with 119 vertical layers (including QBO); dashed line denotes model version with 67 vertical layers (without QBO) as presented by Schmidt et al. [2006]. Results have been normalized as in Figure 1. Error bars indicate the 1σ range around the response at a given model level.

more than 2%/100 sfu is simulated around 5 hPa (~ 36 km) with relatively little latitudinal variation. A secondary maximum of more than 1.5%/100 sfu occurs around 70 hPa (~ 19 km).

[20] Soukharev and Hood [2006] have analyzed observations from three independent satellite instruments. The average tropical vertical profile from these analyses (as presented by Austin et al. [2008]) also indicates a structure with two local maxima. The primary maximum is of similar magnitude as in our simulation but occurs at a higher altitude (corresponding to about 2 hPa). The observed secondary maximum has a larger value of $\sim 3\%$ /100 sfu, but our simulation is within the large error bar of the measurements. The observed latitudinal structure is relatively different for the three satellite instruments [Soukharev and Hood, 2006]. It should be noted that the instruments cover different time periods, and all of these periods have been relatively short (on the order of one solar cycle).

[21] Also the average vertical ozone profile from transient model simulations presented by Austin et al. [2008] shows the primary maximum at a lower altitude than indicated by observations. The reason for this discrepancy between simulations and observations is to our knowledge still unknown. As pointed out by Austin et al. [2008], it might simply be caused by the low vertical resolution of the satellite data. On the basis of 2D-model simulations with and without QBO, McCormack et al. [2007] have suggested that the secondary maximum may be caused by an interaction with the QBO. A comparison of results from the current HAMMONIA simulations with those without QBO presented by Schmidt et al.

[2006] and Schmidt and Brasseur [2006] shows that the equatorial vertical profile does not depend significantly on the inclusion of the QBO (see Figure 3). This is in agreement with the model comparison by Austin et al. [2008], who report that both models with and without QBO may simulate a secondary maximum. However, those simulations were done with time varying observed SSTs. It was suggested that an aliasing effect between solar radiation and SSTs produced or enhanced the apparent solar signal in this region [Austin et al., 2008]. Our results show that a secondary maximum in the lower stratosphere can also be produced in a simulation with climatological SSTs and solar forcing constant in time.

[22] A difficulty in the analysis of observations and transient simulations including several forcing terms is to disentangle solar and QBO signals [Lee and Smith, 2003; Smith and Matthes, 2008]. Salby and Callaghan [2006] have attributed this difficulty to the combined effect of annual and QBO periods leading to a secondary periodicity close to that of the solar cycle. This problem has been circumvented in our simulation by imposing perpetual solar conditions. Smith and Matthes [2008] have suggested that the frequently analyzed upper stratospheric ozone response structure with two local maxima at midlatitudes [e.g., Randel and Wu, 2007] may be the result of such a contamination of the calculated solar signal by the above mentioned secondary periodicity. Such a two maxima response was analyzed by Smith and Matthes [2008] only in the case of a simulation forced to the observed QBO and not from simulations with an idealized sinusoidal QBO or without QBO. Hence, our simulated response with little latitudinal variation may be close to the “pure” solar signal.

3.2. Stratospheric Response During Northern Hemisphere Winter

[23] Figure 4 shows the temporal evolution of monthly mean zonal mean winds, their standard deviations and their differences between solar maximum and minimum for the NH winter months November to March. In November, a statistically significant positive solar cycle effect extends from the subtropical jet in the stratopause region toward higher latitudes in the midstratosphere. The maximum response is of about 7 m/s. Also from December to February, a positive response is simulated in large parts of the polar vortex region in the midlatitude to high-latitude stratosphere. But it is statistically significant at the 95% level only in the lower stratosphere around 60°N to 70°N for January and February. In the upper stratosphere the year to year variability expressed by the standard deviation is much larger than the signal. With respect to the simulations without QBO [Schmidt and Brasseur, 2006], there is now a stronger positive effect on the polar night jet. However, in large regions both simulations show insignificant signals. The background zonal wind has changed relatively little with respect to the simulations by Schmidt and Brasseur [2006], but the QBO causes a weak increase of the variability in mid to high latitudes, and, of course, a strong increase in the equatorial stratosphere.

[24] The wind response analyzed from NCEP/NCAR [e.g., Kodera and Kuroda, 2002] and ECMWF ERA40 [e.g., Berg et al., 2007] reanalysis data shows a poleward and downward propagation of a positive zonal wind response during the course of NH winter and a weakening of the stratospheric polar night jet in late winter. This behavior that can be ex-

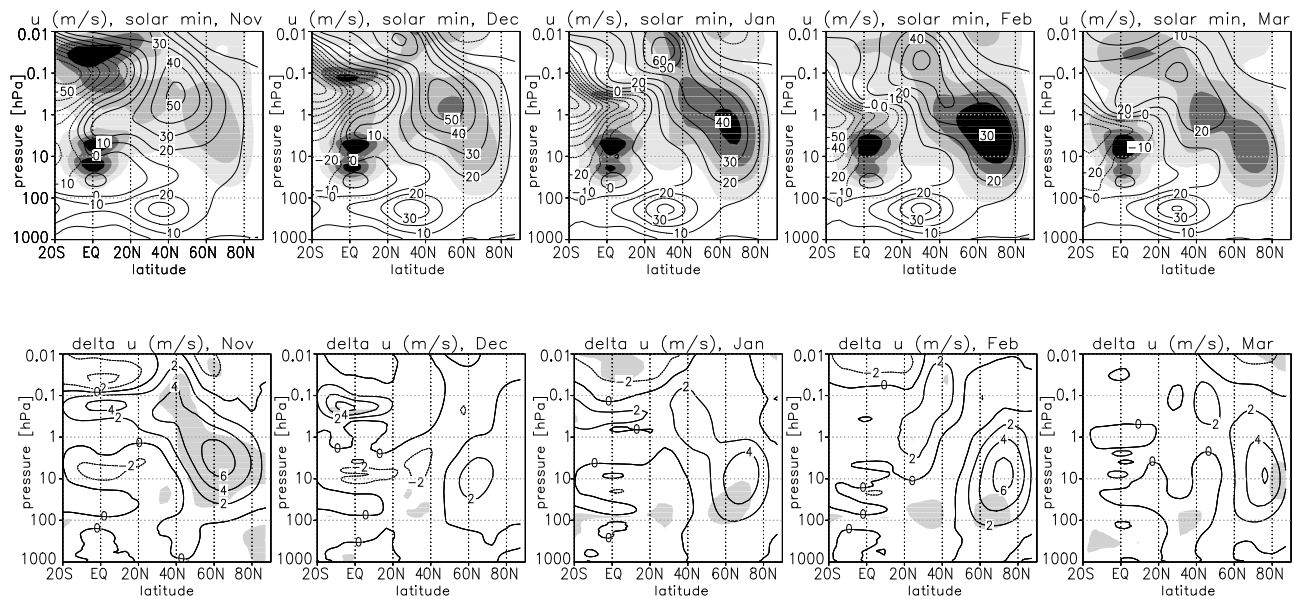


Figure 4. (top) Contours indicate monthly and zonal average zonal wind (m/s) for the NH winter months November to March from the solar minimum simulation. Gray shading indicates standard deviations larger than 4, 8, 12, and 16 m/s (from light to dark). (bottom) Contours indicate monthly and zonal average differences in zonal wind (m/s) between solar maximum and solar minimum. Gray shading marks the regions where the statistical significance of the difference is larger than 95%.

plained by the interaction of zonal winds and planetary waves cannot be observed in Figure 4. However, wind anomalies of single winters show such a behavior but at very different times. Therefore, this is not visible in the winter average. One reason may be that HAMMONIA produces a relatively high polar night jet variability already in November. Compared to reanalysis data presented by *Matthes et al.* [2003, Figure 10], our simulated standard deviation around 60°N in the stratosphere is higher by about 2 to 4 m/s. This high variability is also evident from the higher than observed occurrence rate of sudden stratospheric warmings in November (see section 4.4).

[25] However, the increase of the NH winter polar night jet during solar maximum is statistically significant if the signal is averaged over any three months from November to March. According to *Kodera and Kuroda* [2002] the solar signal in

the upper stratosphere should be transported downward via two pathways: the poleward downward movement of the wind anomaly and a weakening of the meridional circulation leading to the secondary response maximum in the equatorial lower stratosphere. In the following we check the plausibility of the latter mechanism using model data for November. *Kodera and Kuroda* [2002] proposed that the mechanism starts with an increased solar heating in the sunlit latitudes of the stratopause region. This can be identified in the model (see Figure 5). Via the thermal wind relation this leads to increased zonal winds (Figure 4). Thereby, the propagation conditions for planetary waves and their momentum deposition are changed. This can be seen in Figure 5 from the positive EP flux anomaly over a large vertical extension of northern mid to high latitudes. However, in the model this signal is significant only in the lower mesosphere. This wave

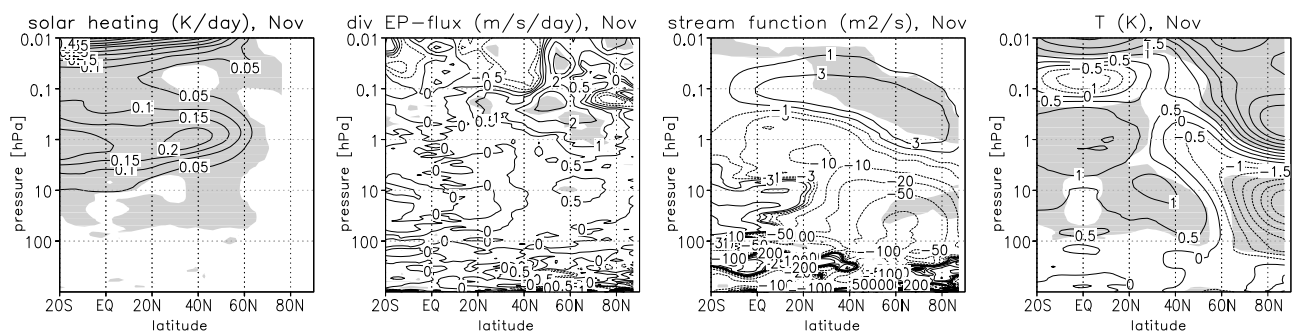


Figure 5. Contours indicate November monthly and zonal average differences between the solar maximum and minimum simulations for (from left to right) solar short wave heating (K/d), EP flux divergence (m/s/d), stream function (m^2/s), and temperature (K). Gray shading marks the regions where the statistical significance of the difference is larger than 95%.

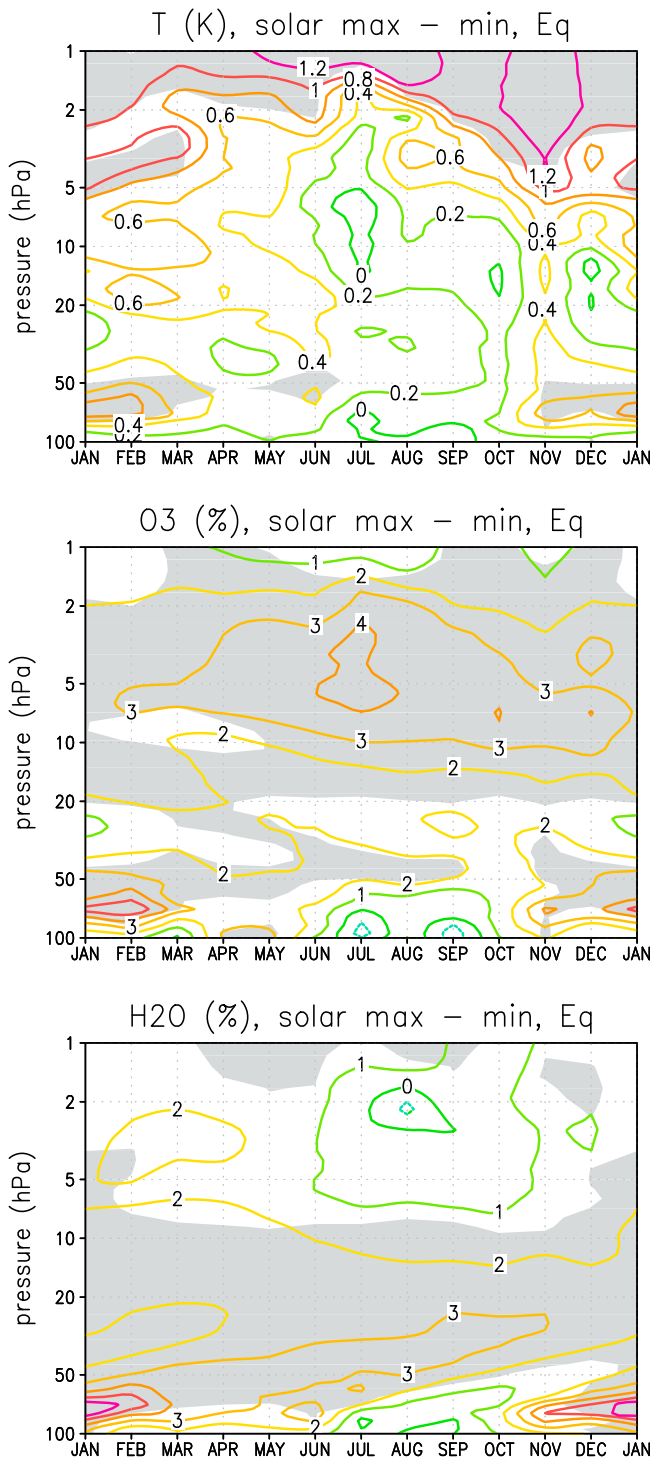


Figure 6. Average annual cycle equatorial zonal average difference between solar maximum and solar minimum for (top) temperature (K) and (middle) ozone and (bottom) water vapor volume mixing ratios (in percent with respect to solar minimum). Gray shading marks the regions where the statistical significance of the difference is larger than 95%.

forcing should modify the meridional circulation by slowing the Brewer-Dobson circulation with its upwelling in equatorial and downwelling in high latitudes. Such a reduced meridional circulation during solar maximum is produced by

the model (see stream function in Figure 5). It is however difficult to assess how strongly the change in the planetary wave momentum deposition contributes to the change of the meridional circulation. It is also impossible to unambiguously distinguish cause and effect in the wave-mean flow interaction because the changed wave forcing will feed back on the mean flow. We are more certain that the reduced equatorial upwelling is indeed causing the simulated positive temperature response in the lower equatorial stratosphere (see next paragraph). It should be noted that in other winter months some of the steps in this mechanism can be traced less well in the model response to solar forcing, and our analysis in this paragraph neglects the temporal evolution of the response. Nevertheless, we think our simulation confirms the plausibility of the mechanism proposed by *Kodera and Kuroda* [2002].

[26] Figure 6 shows the annual cycle of the equatorial stratospheric response to solar cycle forcing in temperature, ozone and water vapor. The positive response in temperature and ozone around 70 hPa is indeed a NH wintertime feature. It is significant from about November to February. One might guess that the NH winter maximum in temperature is at least partly a response to the ozone response via increased absorption of solar radiation. An analysis of the energy balance (not shown) however indicates that the effect of increased absorption is negligible at this altitude, and that both parameters, temperature and ozone mixing ratio, respond directly to the decrease in upwelling. The same is true for water vapor which might not only be influenced by a change in upwelling but also by even small solar effects on the tropopause temperature. Independent of the reason for the increase in the lower stratosphere, this anomaly is transported by the equatorial upwelling and can be identified over a large altitude and time range.

[27] Figure 6 shows a significant positive response of ozone in the lower stratosphere also in SH winter. The response maximum is weaker and occurs higher (at about 50 hPa) than in NH winter. A reason for this weaker SH response may be that also the increase of the polar night jet is on average weaker in the simulated SH winter than in NH winter.

3.3. Tropospheric Response

[28] Figure 7 shows the response of tropospheric zonal winds to solar forcing as an average for the NH winter months December to February. The only regions with a significant response are the Southern Hemisphere subtropics to mid-latitudes. The zonal wind increases close to 45°S over an altitude range from the boundary layer to the tropopause. The maximum increase is of about 0.8 m/s close to about 200 hPa. Equatorward of this is a region of weaker zonal westerly wind with a maximum decrease of about -0.8 m/s close to 25°S and 200 hPa. This response pattern can be interpreted as a poleward shift of the subtropical westerly jet in the Southern Hemisphere. The simulated response can be compared to an analysis of ECMWF ERA40 data by *Crooks and Gray* [2005, Figure 7] which is very similar but the maxima have about twice the simulated magnitude. *Haigh and Blackburn* [2006] have simulated a very similar response pattern in a general circulation model where they imposed an artificial heat source in the lower equatorial stratosphere. They explained the downward propagation of the signal by a change in the

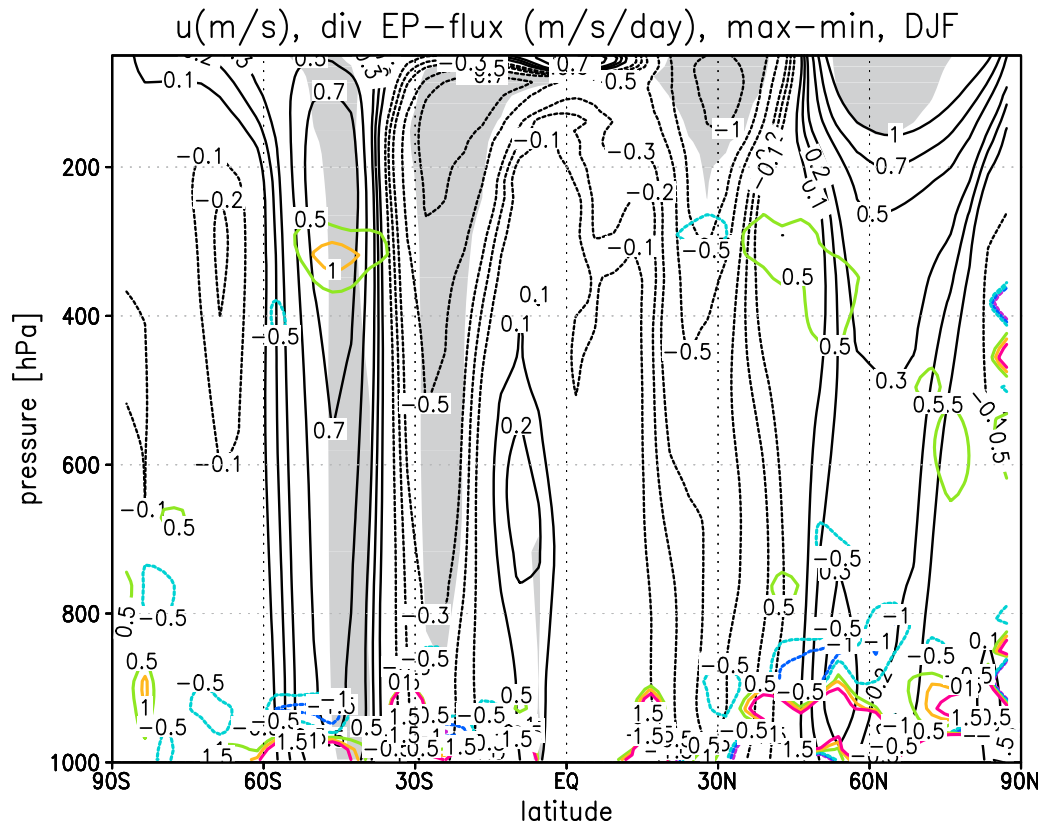


Figure 7. Northern Hemisphere winter (December-January-February) and zonal average difference between solar maximum and solar minimum for zonal wind (m/s, black contours) and EP flux divergence (m/s/d, colored contours). Gray shading marks the regions where the statistical significance of the difference in zonal wind is larger than 95%.

static stability of the tropopause region and a subsequent weakening of the poleward eddy momentum flux convergence. They were reporting however that the details of the mechanism involved in the signal propagation from the stratosphere to the troposphere are still unclear. It is also difficult to assess them from our simulation. But the change in the momentum forcing of the eddy flux reported by *Haigh and Blackburn* [2006] can also be identified in our simulation. It can be identified in Figure 7 as EP flux change at the center of the SH zonal wind increase.

4. Analysis of the Solar Cycle Signal in the Different QBO Phases

4.1. QBO in HAMMONIA

[29] In order to assess possible reasons for success or failure to reproduce solar cycle-QBO interactions in the HAMMONIA it is first necessary to analyze in how far the model is able to reproduce a realistic QBO. *Giorgetta et al.* [2006] have thoroughly analyzed the climatology and the forcing of the QBO in the MAECHAM5 GCM, and evaluated it against ECMWF ERA40 data. As the HAMMONIA is based on MAECHAM5, also its QBO characteristics are very similar. Figure 8 shows the evolution of monthly averaged equatorial zonal winds for 20 years of the solar maximum simulation. The stratospheric winds are dominated by a characteristic QBO pattern while above about 3 hPa the semiannual oscillation is the most prominent feature. One

may compare this with radiosonde observations of zonal winds at Singapore (also shown in Figure 8) or with a similar figure for 20 year of zonal winds from ERA40 data as presented by Figure 3 of *Giorgetta et al.* [2006]. Most prominent differences are that the simulated westerly phase reaches only down to an altitude corresponding to about 70 hPa while in the reanalysis data and in the observations it reaches sometimes an altitude corresponding to 100 hPa, and the somewhat too small simulated amplitude (and in particular too low maximum wind speed in the easterly phase) between about 20 and 50 hPa. Those weaknesses are shared with the MAECHAM5 QBO. Another difference to the observed QBO is the length of the QBO period. The average observed value is of about 28 months while in HAMMONIA it is apparently tightly coupled to the annual cycle (except for one QBO cycle in the solar minimum simulation) which leads to a period of about 24 months. Figure 9 shows vertical profiles of simulated zonal winds for the months of November, January, and March, averaged for the QBO-w and QBO-e cases. For QBO-e, the maximum easterly wind speed occurs at or above 20 hPa, and not at 30 hPa as one would expect from choosing this pressure level to define the QBO criterion (see section 2). The upward shift of the maximum is due to the unrealistic simulated QBO period of 24 months leading to a preferential occurrence of specific QBO phases at specific seasons. The QBO period simulated with HAMMONIA is in contrast to a comparable MAECHAM5 simulation with the same horizontal resolution that produces a 26 month period. Differ-

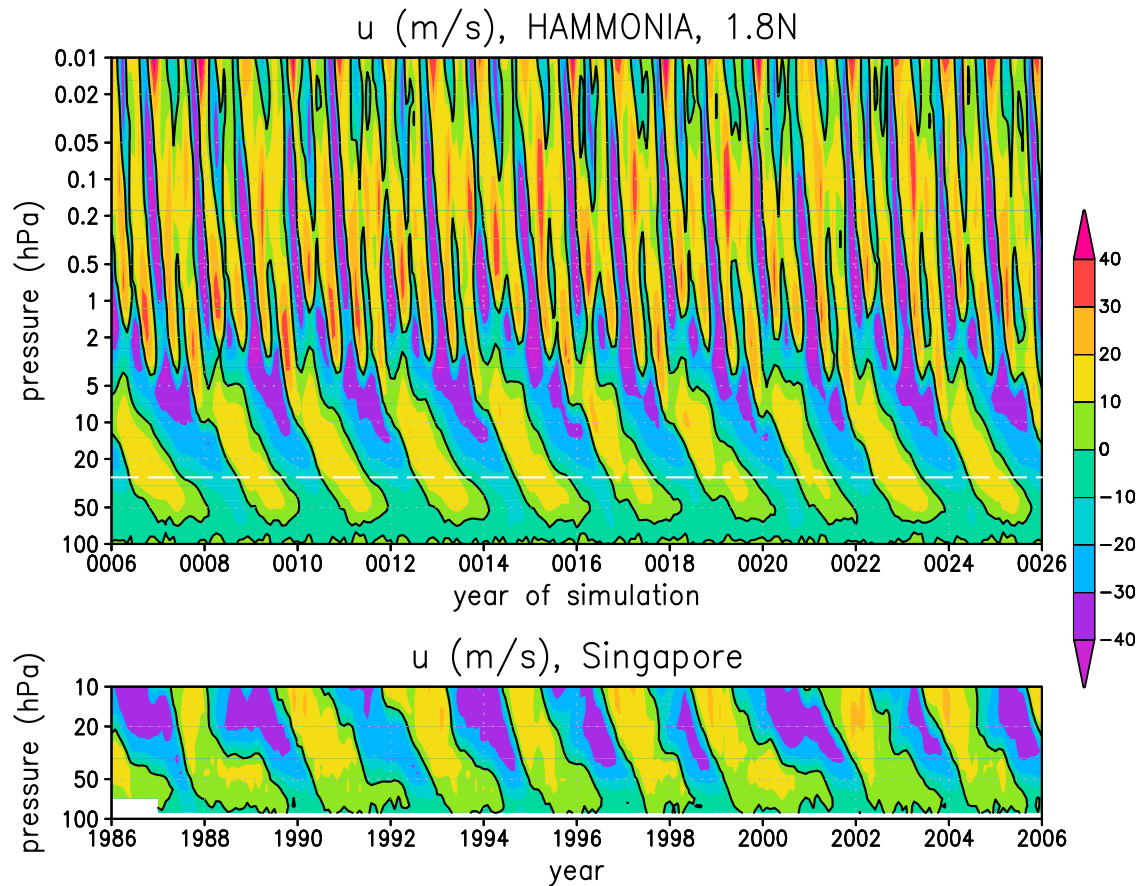


Figure 8. (top) Zonal average zonal wind (m/s) at 1.8°N during 20 years of the solar maximum simulation. The dashed white line at 30 hPa indicates the level that is used to define QBO-w and QBO-e phases. (bottom) Monthly averaged zonal wind (m/s) observed by radiosondes at Singapore (1°N, 104°E) in the years 1986 to 2005.

ences between HAMMONIA and ECHAM5 may be due to the interactive chemistry in HAMMONIA that may change the QBO period via an ozone feedback [see, e.g., *Butchart et al.*, 2003]. A more realistic period might also be achieved with a better horizontal resolution. An MAECHAM5 simulation with a T42 spectral truncation shows a 3 month longer average period than the T31 simulation [*Giorgetta et al.*, 2006]. Another difference between HAMMONIA and ERA40 data is that the latitudinal width of the westerly QBO phase is slightly too small.

[30] A modulation of the QBO period by the solar cycle was observed by *Salby and Callaghan* [2000] and simulated in a 2D model by *McCormack et al.* [2007]. They report a shorter duration of the westerly QBO phase during solar maximum than during solar minimum. Although the HAMMONIA QBO is internally produced it does not show such a feature.

4.2. Dependence of the QBO Signal on the Solar Cycle

[31] The interdependence of the QBO and solar cycle signals can be interpreted in two directions: view a, where the QBO signal is modulated by the solar cycle, and view b, where the solar cycle signal is modulated by the QBO. Figure 10 is intended for studying view a. It shows the dif-

ference of zonally averaged zonal winds between QBO-e and QBO-w (see section 2 for the definition of the phases) for the months of January to March and for both solar maximum and solar minimum conditions. In the equatorial region, the wind difference shows the QBO itself with in general three cells (phases) in the stratosphere. This is very similar to what, for example, *Gray et al.* [2004] and *Lu et al.* [2008] have analyzed. During January and February the QBO influence on higher latitudes is very similar for solar minimum and maximum showing an insignificantly weaker polar vortex during QBO-e than QBO-w. In an analysis of the QBO signal for all cases (independent of the solar forcing) the signal becomes significant. This is the Holton-Tan relationship [*Holton and Tan*, 1980, 1982]. However, as pointed out in section 1, observations indicate that the Holton-Tan relationship holds mainly in the early winter months. During November and December, our simulations show no significant QBO influence on the extratropical zonal wind. In January and February, no significant difference between solar maximum and minimum is simulated. This changes, however, in March, where no significant QBO dependence of the zonal wind in the extratropics can be identified during solar minimum. During solar maximum, however, zonal westerlies are stronger by more than 10 m/s from the midlatitude lower

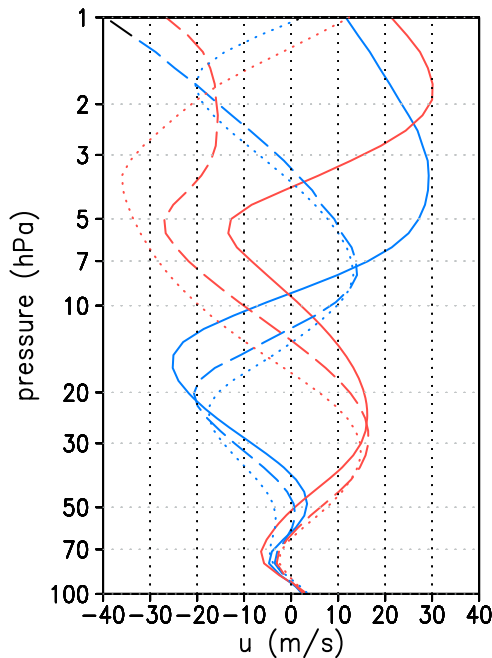


Figure 9. Vertical profiles of monthly and zonally averaged simulated zonal winds (m/s) at 1.8°N for the months of November (solid line), January (dashed line), and March (dotted line). Blue (red) indicates the average profiles for the QBO-e (QBO-w) phase.

mesosphere to the polar midstratosphere. The earlier winter months November and December are not shown, here, because the extratropical wind signals are mostly insignificant.

[32] The simulated signals may be compared to the QBO signals in ECMWF reanalysis and operational data analyzed by *Lu et al.* [2008] for the period 1958–2006 (see their Figure 6). Their analysis independent of the solar cycle phase also shows the weaker vortex in January and February for the QBO-e phase. This effect is much weaker in the period 1977–1997 than in the periods before 1977 and after 1997. In March, the signal depends even more strongly on the analyzed period. The QBO-e vortex is stronger than the QBO-w vortex for the period 1977–1997 but weaker in the two periods before and after. The signal for 1977–1997 looks similar to our simulated March signal for solar maximum. *Lu et al.* [2008] do not show a solar cycle-dependent QBO signal for March. For the months of January and February they confirm the earlier finding by, for example, *Labitzke and van Loon* [1988] and *Gray et al.* [2001] that the Holton-Tan relationship is significant only during solar minimum. Our model does not show this.

4.3. Dependence of the Solar Cycle Signal on the QBO

[33] The dependence of the solar cycle signal on the QBO phase is shown in Figures 11 (zonal wind) and 12 (temperature), again for the months of January to March. The zonal wind response to solar forcing in January and February does not differ strongly between QBO-e and QBO-w. In both phases, the polar vortex is slightly stronger during the maximum phase as already seen in Figure 4. For the month of March the solar signals differ between the QBO phases.

During QBO-w the polar vortex is significantly stronger in the solar maximum phase than in the minimum phase; during QBO-e, the signal is of opposite sign but not statistically significant. The temperature and wind signals are linked via the thermal wind relation. The high-latitude solar cycle temperature response during most winter months and QBO phases is negative from the lower to mid stratosphere and positive in the upper stratosphere and lower mesosphere. The statistical significance of these signals is low except for March during QBO-w. In March during QBO-e a positive (but insignificant) high-latitude signal occurs in the midstratosphere. The differences in March may also be interpreted as a shift in the average timing of the final stratospheric warming. Figure 13 shows the time evolution of the polar night jet zonal wind at 60°N and 10 hPa for all four combinations of solar cycle and QBO phases. All through late winter, after the beginning of March, the zonal wind for solar maximum and QBO-e is stronger than in the three other cases and turns to easterlies almost 10 days later in the middle of April.

[34] *Matthes et al.* [2004] show a QBO-dependent analysis of the solar effect on zonal winds in NCEP/NCAR reanalysis data from 1979 to 1997. During QBO-w the poleward downward propagation of the positive wind anomaly happens earlier than during QBO-e, so that in February a negative anomaly is observed for the entire midlatitude to high-latitude stratosphere while during QBO-e a positive anomaly is still observed in the lower stratosphere. Although the poleward downward signal propagation is not apparent in the averaged HAMMONIA simulations (see section 3.2), the simulated dependence of the solar signal on the QBO in March agrees with the observed one in February. In observations, one clear QBO dependence of the solar cycle signal is the positive correlation of the 30 hPa North pole temperature in February with the solar cycle during QBO-w. During QBO-e the correlation is slightly negative but of low significance. This was reported by *Labitzke and van Loon* [1988] and confirmed later using longer time series, for example, by *Labitzke* [2005]. The HAMMONIA simulation shows a qualitatively similar dependence in March. It can be summarized that the simulated and observed time evolutions of the solar signal and its QBO dependence differ strongly.

4.4. Discussion

[35] It is difficult to understand why the model shows only a weak QBO dependence of the solar cycle during most winter months but a strong one in March. Generally, the QBO effect on zonal winds in the winter hemisphere is associated with interactions between planetary waves and the mean flow. The QBO modulates the position of the zero-wind line and thereby the waveguide for planetary waves. Via the thermal wind relation the solar cycle has a direct influence on zonal winds in the stratopause region. Therefore, the suggestion of, for example, *Gray et al.* [2004] that the solar cycle-QBO relation depends strongly on winds in the upper equatorial stratosphere, where QBO and solar influences may enhance or counteract each other, seems plausible. However, the detection of possible mechanisms responsible for this behavior is difficult from our model simulations. One reason for this is the apparent very slow poleward downward signal propagation in HAMMONIA. Individual anomalies propa-

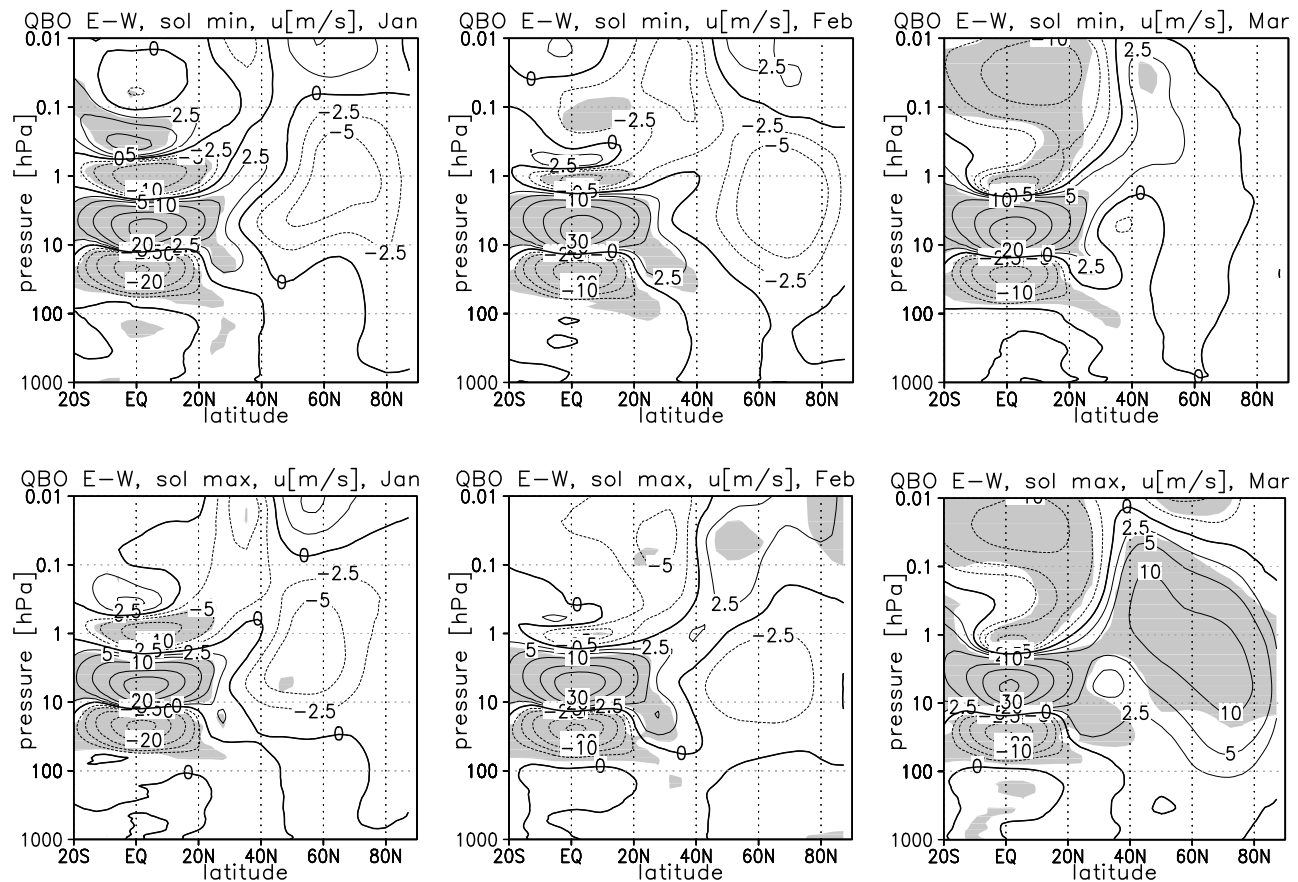


Figure 10. Contours indicate monthly and zonal average differences in zonal wind (m/s) between seasons with QBO east and west conditions for (left) January, (middle) February, and (right) March. Solar (top) minimum and (bottom) maximum conditions. See text for the exact QBO criterion. Gray shading marks the regions where the statistical significance of the difference is larger than 95%.

gate realistically, but as the anomalies start to propagate at very different times during winter, the resulting propagation is slow.

[36] One important process in the NH winter response to solar and QBO forcing are sudden stratospheric warmings (SSWs) [see, e.g., McIntyre, 1982; Gray *et al.*, 2004; Lu *et al.*, 2008]. Gray *et al.* [2004] have analyzed changes in the occurrence frequency of SSW for the different QBO–solar cycle combinations and reported, for example, that in February under QBO-w, less warmings occur during solar minimum than during solar maximum. This relationship is not reproduced by our model. While several models have significantly different occurrence frequencies of SSWs than reanalysis data [Charlton *et al.*, 2007] the average occurrence of SSWs per winter season in HAMMONIA seems to be realistic. Charlton and Polvani [2007] report SSW frequencies of 0.6 and 0.64 per winter in NCEP-NCAR and ECMWF ERA40 reanalysis data, respectively. Our model produces 0.7 warmings per year (0.57 during solar maximum and 0.83 during solar minimum). However, while reanalysis data [Charlton and Polvani, 2007] show only very few warmings occurring in November (about one each 20 years), our model produces a much higher number of these early warmings (about 1 each 7 years). This high variability in early winter may be a cause for the difficulty of the model to reproduce some of the observed features. This should be particularly

true for early winter with the too frequently simulated warmings and midwinter, when the polar vortex is still recovering from the early SSWs.

[37] The dependence of the simulated solar signal in SH winter (not shown) on the QBO is stronger than in NH winter. A poleward downward propagation of the solar signal can be identified in both cases. But this propagation is significantly shifted in time so that the solar signal averaged over both QBO phases appears small. A more detailed presentation of the SH model performance will be presented elsewhere.

5. Summary and Conclusions

[38] We have presented results from HAMMONIA general circulation and chemistry model simulations designed to study the atmospheric response to solar cycle variations and the role of the QBO in this response. Owing to the internally produced QBO, the model is particularly suited for such an exercise. The simulation setup with only solar and QBO forcing allows an unambiguous attribution of the simulated signals. Influences by ENSO, volcanoes, and transient change in greenhouse gases are excluded. The major conclusions from these simulations are:

[39] 1. The model shows a wintertime response in tropospheric zonal winds that resembles strongly the observed response. The strongest direct impact of the solar cycle below

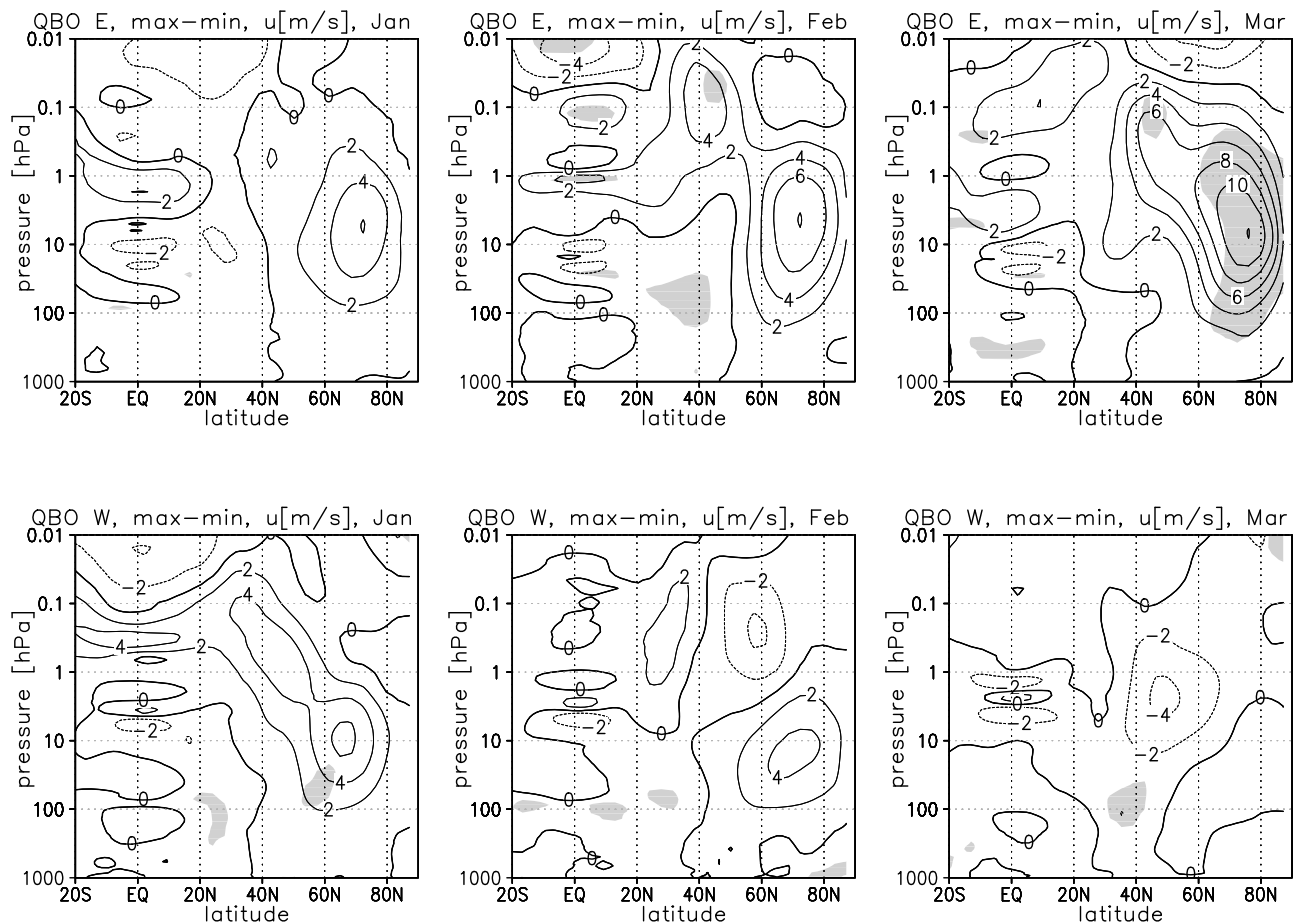


Figure 11. Contours indicate monthly and zonal average differences in zonal wind (m/s) between the solar maximum and minimum simulations for the months of (left) January, (middle) February, and (right) March. QBO (top) east and (bottom) west conditions. See text for the exact QBO criterion. Gray shading marks the regions where the statistical significance of the difference is larger than 95%.

the mesosphere is the additional heating in the stratopause region. The mechanisms suggested by *Kodera and Kuroda* [2002] (transport of the solar signal from the stratopause to the lower equatorial stratosphere) and by *Haigh and Blackburn* [2006] (further downward transport to the troposphere) can be traced qualitatively in the model. Hence the simulations confirm the plausibility of this pathway linking the solar cycle–dependent heating in the stratopause region to the observed tropospheric wind response. We cannot, however, rule out that the troposphere is also directly influenced by the change in total solar radiation as suggested by *Meehl et al.* [2008, 2009]. It may surprise that the tropospheric response to solar forcing seems to be rather well reproduced by the model while many details of the stratospheric response are poorly reproduced. *Haigh and Blackburn* [2006] have simulated a realistic tropospheric response by prescribing a positive temperature anomaly in the lower equatorial stratosphere. Our model produces such a temperature anomaly as a solar response and the mechanism of its production may be unimportant for the downward propagation of the solar signal.

[40] 2. There is an ongoing discussion about the origin of the secondary response maximum in equatorial lower stratospheric ozone and temperature. In contrast to many

other models, HAMMONIA reproduces such a signal in time slice simulations with and without QBO and with climatological SSTs. Future transient simulations with observed SSTs will be performed to test if the secondary maximum can be enhanced in such a setup as it is suggested from some of the model simulations presented by *Austin et al.* [2008]. It is interesting to note that the secondary maximum is reproduced in NH winter although the midlatitude to high-latitude dynamical response shows some discrepancies to the response derived from reanalysis data.

[41] 3. In general, the simulated polar vortex in NH winter is stronger during solar maximum than during solar minimum, as observed. However, the observed poleward downward propagation of the solar signal is much too slow in the simulations. Furthermore, the simulated QBO dependence of the solar signal is insignificant for most winter months. Only in the month of March, solar maximum causes a significantly stronger vortex under QBO–e and a slightly weaker vortex under QBO–w. This is similar to the observed response in February.

[42] The differences between the solar signals in our simulations and reanalysis data may be caused by model deficiencies. The most obvious deficiency is the simulated QBO period of about 2 years rather than 28 months. With this

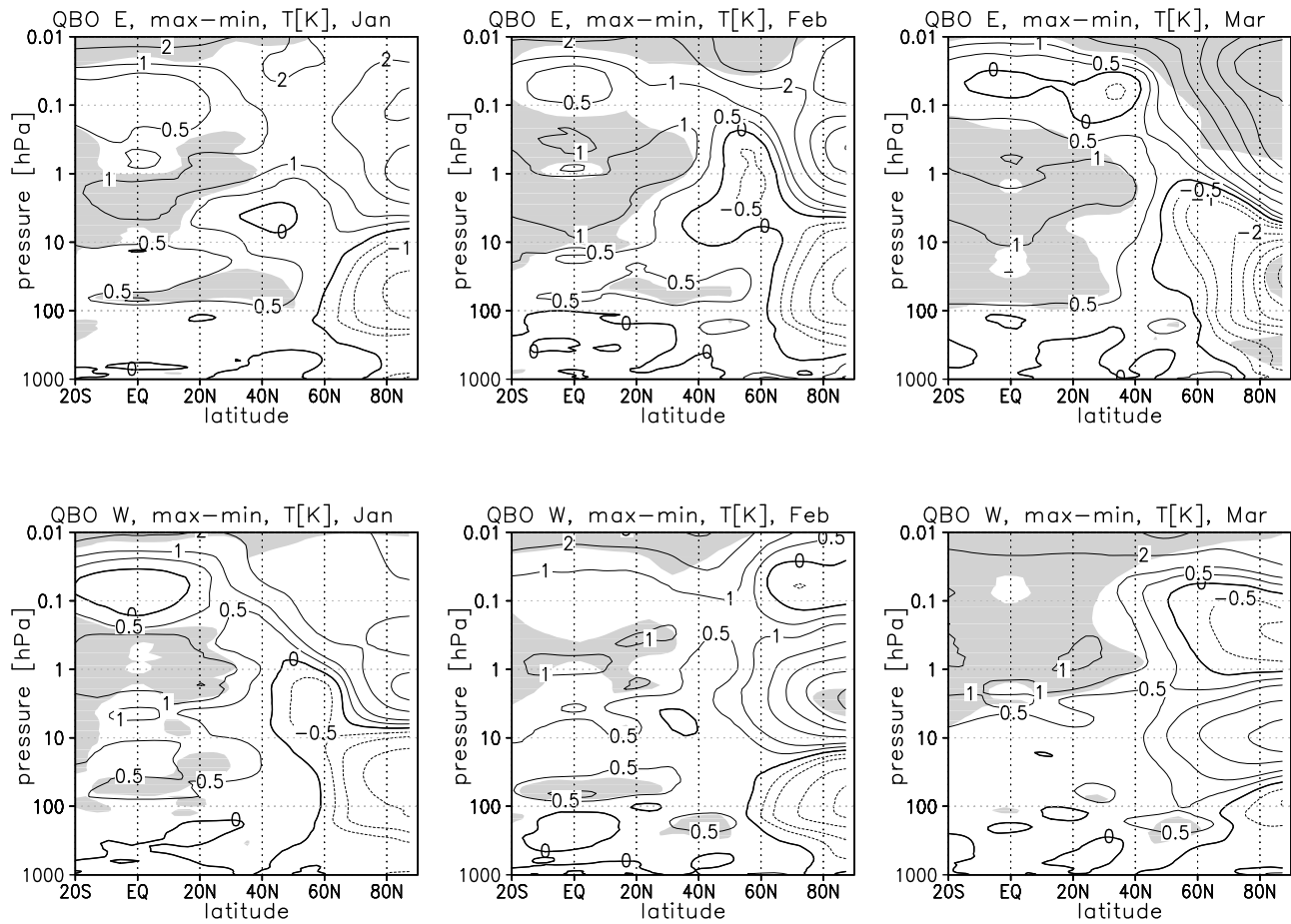


Figure 12. Same as Figures 11 but for temperature (K).

phase locking to the annual cycle, the QBO at a given time of the year and at certain altitudes is always close to a transitional phase and rarely in a clear westerly or easterly phase. It is not yet exactly known which altitudes are the most important ones for the QBO–solar cycle interaction. Although, in general, altitudes between 40 and 50 hPa are chosen to define a QBO criterion, there is some evidence [e.g., *Gray et al.*, 2004; *Matthes et al.*, 2004] for the relevance of upper stratospheric equatorial winds. The relative weakness of the simulated QBO dependence of the solar signal during certain months may be caused by the dominant occurrence of transition phases at important altitudes. Furthermore, the QBO simulated by HAMMONIA does not propagate as far down in the lower stratosphere as it is observed. Very likely this adds to the discrepancies between observed and simulated signals in particular as it prevents us to define the QBO phases at the same pressure level that is used in many observational studies.

[43] *Matthes et al.* [2004] have stressed the importance of a realistic background climatology (both in terms of mean winds and their variability) for the realistic simulation of a response to solar forcing. In this context it is interesting to note that *Lu et al.* [2008] have noticed a change in the Holton–Tan relation with time, and *Kodera et al.* [2008] have derived a solar modulation of NH winter trends attributed to greenhouse gases (which could be interpreted vice versa as a

modulation of the solar signal by climate change). These results suggest that relatively small changes in the background condition may lead to a substantial change in the atmospheric response to solar or other forcing. Hence, a slight deviation of a model’s background climatology from the real atmospheric state for which the response is studied, should produce an unrealistic response. In our case this may in particular apply for early winter, when SSWs are simulated too frequently, and for midwinter when the vortex is still recovering from early winter SSWs.

[44] One way to improve future simulations may be the increase of resolution which is becoming feasible with increasing computer capacities. The increase of vertical resolution with respect to the simulations presented by *Schmidt et al.* [2006], for example, has allowed the simulation of a QBO-like oscillation. *Giorgetta et al.* [2006] have shown that an increased horizontal resolution can lead to a more realistic QBO period. Not only an increase of model resolution but also the use of real climate models (with a coupled ocean model) may help in the simulation of solar signals. The simulations presented by *Marsh and Garcia* [2007] and by *Austin et al.* [2008] have stressed the possible influence of SSTs on the solar response. Many authors (see introduction) have shown solar signals in the troposphere. Furthermore, the simulations by *Berg et al.* [2007] have indicated a solar-like response of the stratosphere to a prescribed tropospheric

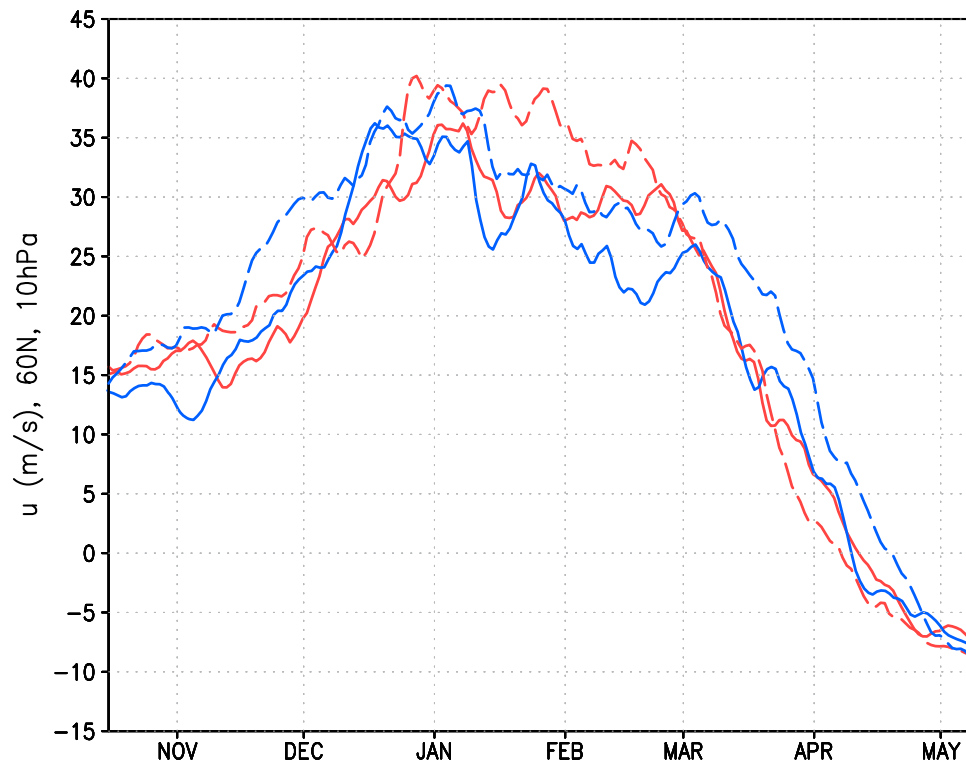


Figure 13. Average time evolution of zonal winds at 60°N and 10 hPa during NH winter for the four combinations of QBO and solar cycle phases. Red is QBO-w, blue is QBO-e, solid line is solar minimum, and dashed line is solar maximum. The ticks on the time axis mark the first day of the respective month.

anomaly. This hints to a possible feedback via the troposphere that would be damped in simulations with fixed SSTs. The use of coupled atmosphere-ocean models would allow the simulation of such feedbacks between the two compartments of the earth system. Recent simulations with WACCM coupled to an ocean model by Meehl *et al.* [2009] indicate, that a more realistic simulation of the solar response in the equatorial Pacific can be obtained in such a coupled model system.

[45] The interdependence of solar signals and QBO signals is not a phenomenon occurring exclusively for these two types of forcing. As mentioned above, Kodera *et al.* [2008] have identified a solar modulation of stratospheric trends attributed to greenhouse gases. Camp and Tung [2007c] and Calvo *et al.* [2009] discuss an interdependence of stratospheric NH winter signals produced by the QBO and by ENSO. They show that, like in the QBO-solar case, the effects of the single forcing types are not necessarily additive. This nonlinearity is a major obstacle in the attribution of observed anomalies in the NH extratropical stratosphere.

[46] **Acknowledgments.** The authors are grateful to Judith Lean, Naval Research Laboratory, Washington, D. C., for providing the solar irradiance spectra. We thank Sebastian Rast and Stergios Misios for carefully reading and correcting the manuscript. We also thank John Austin and two anonymous reviewers for very helpful comments. The simulations with HAMMONIA were performed at the German Climate Computing Center (DKRZ). HAMMONIA studies are supported by the “Deutsche Forschungsgemeinschaft” (DFG) within the CAWSES priority program. This work was initiated during an extended visit of H.S. at the National Center for Atmospheric Research (NCAR).

References

- Achatz, U., N. Grieger, and H. Schmidt (2008), Mechanisms controlling the diurnal solar tide: Analysis using a GCM and a linear model, *J. Geophys. Res.*, *113*, A08303, doi:10.1029/2007JA012967.
- Austin, J., *et al.* (2008), Coupled chemistry climate model simulations of the solar cycle in ozone and temperature, *J. Geophys. Res.*, *113*, D11306, doi:10.1029/2007JD009391.
- Berg, P., B. Christiansen, P. Thejll, and N. Arnold (2007), The dynamical response of the middle atmosphere to the tropospheric solar signal, *J. Geophys. Res.*, *112*, D20122, doi:10.1029/2006JD008237.
- Butchart, N., A. A. Scaife, J. Austin, S. H. E. Hare, and J. R. Knight (2003), Quasi-biennial oscillation in ozone in a coupled chemistry-climate model, *J. Geophys. Res.*, *108*(D15), 4486, doi:10.1029/2002JD003004.
- Calvo, N., M. A. Giorgetta, R. Garcia-Herrera, and E. Manzini (2009), Nonlinearity of the combined warm ENSO and QBO effects on the Northern Hemisphere polar vortex in MAECHAM5 simulations, *J. Geophys. Res.*, *D13109*, doi:10.1029/2008JD011445.
- Camp, C. D., and K. -K. Tung (2007a), The influence of the solar cycle and QBO on the late-winter stratospheric polar vortex, *J. Atmos. Sci.*, *64*, 1267–1283, doi:10.1175/JAS3883.1.
- Camp, C. D., and K. K. Tung (2007b), Surface warming by the solar cycle as revealed by the composite mean difference projection, *Geophys. Res. Lett.*, *34*, L14703, doi:10.1029/2007GL030207.
- Camp, C. D., and K. -K. Tung (2007c), Stratospheric polar warming by ENSO in winter: A statistical study, *Geophys. Res. Lett.*, *34*, L04809, doi:10.1029/2006GL028521.
- Charlton, A. J., and L. M. Polvani (2007), A new look at stratospheric sudden warmings. Part I: Climatology and modeling benchmarks, *J. Clim.*, *20*, 449–469, doi:10.1175/JCLI3996.1.
- Charlton, A. J., L. M. Polvani, J. Perlwitz, F. Sassi, E. Manzini, K. Shibata, S. Pawson, J. E. Nielsen, and D. Rind (2007), A new look at stratospheric sudden warmings. Part II: Evaluation of numerical model simulations, *J. Clim.*, *20*, 470–489, doi:10.1175/JCLI3994.1.
- Charron, M., and E. Manzini (2002), Gravity waves from fronts: Parameterization and middle atmosphere response in a general circulation model, *J. Atmos. Sci.*, *59*, 923–941.
- Crooks, S. A., and L. J. Gray (2005), Characterization of the 11-year solar signal using a multiple regression analysis of the ERA-40 dataset, *J. Clim.*, *18*, 996–1015.

- Eyring, V., et al. (2006), Assessment of temperature, trace species, and ozone in chemistry-climate model simulations of the recent past, *J. Geophys. Res.*, *111*, D22308, doi:10.1029/2006JD007327.
- Eyring, V., et al. (2008), Overview of the new CCMVal reference and sensitivity simulations in support of upcoming ozone and climate assessments and the planned SPARC CCMVal, *SPARC Newsl.*, *30*, 20–26.
- Frame, T. H. A., and L. J. Gray (2010), The 11-year solar cycle in ERA-40 data: An update to 2008, *J. Clim.*, doi:10.1175/2009JCLI13150.1, in press.
- Giorgetta, M. A., E. Manzini, E. Roeckner, M. Esch, and L. Bengtsson (2006), Climatology and forcing of the quasi-biennial oscillation in the MAECHAM5 model, *J. Clim.*, *19*, 3882–3901, doi:10.1175/JCLI3830.1.
- Gleisner, H., and P. Thejll (2003), Patterns of tropospheric response to solar variability, *Geophys. Res. Lett.*, *30*(13), 1711, doi:10.1029/2003GL017129.
- Gray, L. J., S. J. Phipps, T. J. Dunkerton, M. P. Baldwin, E. F. Drysdale, and M. R. Allen (2001), A data study of the influence of the equatorial upper stratosphere on Northern Hemisphere stratospheric sudden warmings, *Q. J. R. Meteorol. Soc.*, *127*, 1985–2004, doi:10.1256/smsqj.57606.
- Gray, L. J., S. Crooks, C. Pascoe, S. Sparrow, and M. Palmer (2004), Solar and QBO influences on the timing of stratospheric sudden warmings, *J. Atmos. Sci.*, *61*, 2777–2796.
- Gruzdev, A. N., H. Schmidt, and G. P. Brasseur (2009), The effect of the solar rotational irradiance variation on the middle and upper atmosphere calculated by a three-dimensional chemistry-climate model, *Atmos. Chem. Phys.*, *9*, 595–614.
- Haigh, J. D. (1999), A gcm study of climate change in response to the 11-year solar cycle, *Q. J. R. Meteorol. Soc.*, *125*, 871–892, doi:10.1002/qj.4971255506.
- Haigh, J. D., and M. Blackburn (2006), Solar influences on dynamical coupling between the stratosphere and troposphere, *Space Sci. Rev.*, *125*, 331–344.
- Haigh, J., M. Blackburn, and R. Day (2005), The response of tropospheric circulation to perturbations in lower-stratospheric temperature, *J. Clim.*, *18*, 3672–3685.
- Hamilton, K. (2002), On the quasi-decadal modulation of the stratospheric QBO period, *J. Clim.*, *15*, 2562–2565, doi:10.1175/1520-0442(2002)015.
- Hines, C. O. (1997a), Doppler-spread parameterization of gravity wave momentum deposition in the middle atmosphere. Part 1: Basic formulation, *J. Atmos. Sol. Terr. Phys.*, *59*, 371–386.
- Hines, C. O. (1997b), Doppler-spread parameterization of gravity wave momentum deposition in the middle atmosphere. Part 2: Broad and quasi-monochromatic spectra, and implementation, *J. Atmos. Sol. Terr. Phys.*, *59*, 387–400.
- Holton, J. R., and H. C. Tan (1980), The influence of the equatorial quasi-biennial oscillation on the global circulation at 50 mb, *J. Atmos. Sci.*, *37*, 2200–2208.
- Holton, J. R., and H. C. Tan (1982), The quasi-biennial oscillation in the Northern Hemisphere lower stratosphere, *J. Meteorol. Soc. Jpn.*, *60*, 140–148.
- Kinnison, D. E., et al. (2007), Sensitivity of chemical tracers to meteorological parameters in the MOZART-3 chemical transport model, *J. Geophys. Res.*, *112*, D20302, doi:10.1029/2006JD007879.
- Kodera, K., and Y. Kuroda (2002), Dynamical response to the solar cycle, *J. Geophys. Res.*, *107*(D24), 4749, doi:10.1029/2002JD002224.
- Kodera, K., and K. Shibata (2006), Solar influence on the tropical stratosphere and troposphere in the northern summer, *Geophys. Res. Lett.*, *33*, L19704, doi:10.1029/2006GL026659.
- Kodera, K., M. E. Hori, S. Yukimoto, and M. Sigmond (2008), Solar modulation of the Northern Hemisphere winter trends and its implications with increasing CO₂, *Geophys. Res. Lett.*, *35*, L03704, doi:10.1029/2007GL031958.
- Labitzke, K. (1987), Sunspots, the QBO, and the stratospheric temperature in the north polar region, *Geophys. Res. Lett.*, *14*, 535–537, doi:10.1029/GL014i005p00535.
- Labitzke, K. (2005), On the solar cycle-QBO relationship: A summary, *J. Atmos. Sol. Terr. Phys.*, *67*, 45–54.
- Labitzke, K., and H. van Loon (1988), Associations between the 11-year solar cycle, the QBO and the atmosphere, part I: The troposphere and the stratosphere in the Northern Hemisphere winter, *J. Atmos. Sol. Terr. Phys.*, *64*, 203–210.
- Labitzke, K., J. Austin, N. Butchart, J. Knight, M. Takahashi, M. Nakamoto, T. Nagashima, J. Haigh, and V. Williams (2002), The global signal of the 11-year solar cycle in the stratosphere: Observations and models, *J. Atmos. Sol. Terr. Phys.*, *64*, 203–210.
- Lean, J. (2000), Evolution of the Sun's spectral irradiance since the Maunder Minimum, *Geophys. Res. Lett.*, *27*, 2425–2428.
- Lee, H., and A. K. Smith (2003), Simulation of the combined effects of solar cycle, quasi-biennial oscillation, and volcanic forcing on stratospheric ozone changes in recent decades, *J. Geophys. Res.*, *108*(D2), 4049, doi:10.1029/2001JD001503.
- Lu, H., M. P. Baldwin, L. J. Gray, and M. J. Jarvis (2008), Decadal-scale changes in the effect of the QBO on the northern stratospheric polar vortex, *J. Geophys. Res.*, *113*, D10114, doi:10.1029/2007JD009647.
- Manzini, E., M. A. Giorgetta, M. Esch, L. Kornbluh, and E. Roeckner (2006), The influence of sea surface temperatures on the northern winter stratosphere: Ensemble simulations with the MAECHAM5 model, *J. Clim.*, *19*, 3863–3881.
- Marsh, D. R., and R. R. Garcia (2007), Attribution of decadal variability in lower-stratospheric tropical ozone, *Geophys. Res. Lett.*, *34*, L21807, doi:10.1029/2007GL030935.
- Matthes, K., K. Kodera, J. D. Haigh, D. T. Shindell, K. Shibata, U. Langematz, and E. Rozanov (2003), GRIPS solar experiments intercomparison project: Initial results, *Pap. Meteorol. Geophys.*, *54*, 71–90.
- Matthes, K., U. Langematz, L. J. Gray, K. Kodera, and K. Labitzke (2004), Improved 11-year solar signal in the Freie Universität Berlin Climate Middle Atmosphere Model (FUB-CMAM), *J. Geophys. Res.*, *109*, D06101, doi:10.1029/2003JD004012.
- Matthes, K., Y. Kuroda, K. Kodera, and U. Langematz (2006), Transfer of the solar signal from the stratosphere to the troposphere: Northern winter, *J. Geophys. Res.*, *111*, D06108, doi:10.1029/2005JD006283.
- McCormack, J. P., D. E. Siskind, and L. L. Hood (2007), Solar-QBO interaction and its impact on stratospheric ozone in a zonally averaged photochemical transport model of the middle atmosphere, *J. Geophys. Res.*, *112*, D16109, doi:10.1029/2006JD008369.
- McIntyre, M. E. (1982), How well do we understand the dynamics of stratospheric warmings?, *J. Meteorol. Soc. Jpn.*, *60*, 37–65.
- Meehl, G. A., J. M. Arblaster, G. Branstator, and H. van Loon (2008), A coupled air-sea response mechanism to solar forcing in the Pacific region, *J. Clim.*, *21*, 2883–2897.
- Meehl, G. A., J. M. Arblaster, K. Matthes, F. Sassi, and H. van Loon (2009), Amplifying the Pacific climate system response to a small 11-year solar cycle forcing, *Science*, *325*, 1114–1118, doi:10.1126/science.1172872.
- Naito, Y., and I. Hirota (1997), Interannual variability of the northern winter stratospheric circulation related to the QBO and the solar cycle, *J. Meteorol. Soc. Jpn.*, *75*, 925–937.
- Offermann, D., M. Jarisch, H. Schmidt, J. Oberheide, K. U. Grossmann, O. Gusev, J. M. Russell III, and M. G. Mlyneczek (2007), The “wave turbopause,” *J. Atmos. Sol. Terr. Phys.*, *69*, 2139–2158, doi:10.1016/j.jastp.2007.05.012.
- Offermann, D., O. Gusev, M. Donner, J. M. Forbes, M. Hagan, M. G. Mlyneczek, J. Oberheide, P. Preusse, H. Schmidt, and J. M. Russell III (2009), Relative intensities of middle atmosphere waves, *J. Geophys. Res.*, *114*, D06110, doi:10.1029/2008JD010662.
- Punge, H. J., and M. A. Giorgetta (2008), Net effect of the QBO in a chemistry climate model, *Atmos. Chem. Phys.*, *8*, 6505–6525.
- Randel, W. J., and F. Wu (2007), A stratospheric ozone profile data set for 1979–2005: Variability, trends, and comparisons with column ozone data, *J. Geophys. Res.*, *112*, D06313, doi:10.1029/2006JD007339.
- Randel, W. J., et al. (2009), An update of observed stratospheric temperature trends, *J. Geophys. Res.*, *114*, D02107, doi:10.1029/2008JD010421.
- Richards, P. G., J. A. Fennelly, and D. G. Torr (1994), A solar EUV flux model for aeronomic calculations, *J. Geophys. Res.*, *99*, 8981–8992. (Correction, *J. Geophys. Res.*, *99*, 13,283, 1994.)
- Roeckner, E., R. Brokopf, M. Esch, M. Giorgetta, S. Hagemann, L. Kornbluh, E. Manzini, U. Schlese, and U. Schulzweida (2006), Sensitivity of simulated climate to horizontal and vertical resolution in the ECHAM5 atmosphere model, *J. Clim.*, *19*, 3771–3791.
- Salby, M., and P. Callaghan (2000), Connection between the solar cycle and the QBO: The missing link, *J. Clim.*, *13*, 2652–2662.
- Salby, M. L., and P. F. Callaghan (2006), Relationship of the quasi-biennial oscillation to the stratospheric signature of the solar cycle, *J. Geophys. Res.*, *111*, D06110, doi:10.1029/2005JD006012.
- Schmidt, H., and G. P. Brasseur (2006), The response of the middle atmosphere to solar cycle forcing in the Hamburg Model of the Neutral and Ionized Atmosphere, *Space Sci. Rev.*, *125*(1–4), 345–356, doi:10.1007/s11214-006-9068-z.
- Schmidt, H., et al. (2006), The HAMMONIA chemistry climate model: Sensitivity of the mesopause region to the 11-year solar cycle and CO₂ doubling, *J. Clim.*, *19*, 3903–3931.
- Smith, A. K., and K. Matthes (2008), Decadal-scale periodicities in the stratosphere associated with the solar cycle and the QBO, *J. Geophys. Res.*, *113*, D05311, doi:10.1029/2007JD009051.
- Soukharev, B. E., and L. L. Hood (2006), Solar cycle variation of stratospheric ozone: Multiple regression analysis of long-term satellite data sets and comparisons with models, *J. Geophys. Res.*, *111*, D20314, doi:10.1029/2006JD007107.

van Loon, H., G. A. Meehl, and D. J. Shea (2007), Coupled air-sea response to solar forcing in the Pacific region during northern winter, *J. Geophys. Res.*, *112*, D02108, doi:10.1029/2006JD007378.

Yuan, T., H. Schmidt, C. Y. She, D. A. Krueger, and S. Reising (2008), Seasonal variations of semidiurnal tidal perturbations in mesopause region temperature and zonal and meridional winds above Fort Collins,

Colorado (40.6°N, 105.1°W), *J. Geophys. Res.*, *113*, D20103, doi:10.1029/2007JD009687.

G. P. Brasseur, Climate Service Center, Bundesstr. 45a, D-20146 Hamburg, Germany.

M. A. Giorgetta and H. Schmidt, Max Planck Institute for Meteorology, Bundesstr. 53, D-20146 Hamburg, Germany.